5

# TRAPPED ION REGIME

$$\nu_i/\epsilon < \omega < \nu_e/\epsilon \quad , \quad \omega/k_{\parallel} < \left(\epsilon T_i/m_i\right)^{1/2}$$

$$\omega = \omega_f + \sqrt{\epsilon}\,\omega_{*e}/(1+\tau) + i\,\epsilon^2\,\omega_{*e}^2/\nu_e\,(1+\tau)^2$$

## STABILITY FOR +VE FEEDBACK

PHASE 180° GAIN: $\epsilon^2\,\omega_{*e}^2/\nu_e\,(1+\tau)^2$

5

$$n^+ - n^- = \frac{1}{2}\sqrt{\epsilon_0}\, n(r)\sqrt{\rho}\,(\cos\theta + \sqrt{1-\alpha^2})^{1/2}$$

$$\left[\exp\left(-\lambda \frac{\pi - \theta_m - \theta}{\cos\theta + \sqrt{1-\alpha^2}}2\right) - \exp\left(-\lambda \frac{\pi - \theta_m + \theta}{\cos\theta + \sqrt{1-\alpha^2}}2\right)\right]$$

where $\alpha$ is the solution of

$$\left(\frac{2\lambda}{\alpha} - 1\right)(\cos\theta + \sqrt{1-\alpha^2}) = 2\lambda\left(\pi - \theta_m - \frac{q}{|q|}\theta\right)$$

TABLE II

| Experiment | Scaling | $\tau_E$(s) | T(eV) | $\beta_\theta$ | $V_R$(v) |
|---|---|---|---|---|---|
| PLT | A | 0.23 | 1400 | 0.28 | 0.75 |
| R = 1.3 m, a = 0.45 m | B | 0.08 | 920 | 0.19 | 1.43 |
| I = 1 MA, $n_e = 10^{20}$ $m^{-3}$ | C | 0.024 | 570 | 0.12 | 3.0 |
| JET | A | 1.63 | 1300 | 0.30 | 0.59 |
| R = 2.96 m, a = 1.25 m | B | 0.13 | 470 | 0.11 | 3.0 |
| I = 2.6 MA, $n_e = 10^{20}$ $m^{-3}$ | C | 0.014 | 190 | 0.04 | 12 |

4

COLLISIONLESS REGIME ($T_i = T_e$)

$$(\omega - \omega_f)^2 = \omega_M^2 + \sqrt{\epsilon}\,\omega_* \omega_M \quad (\omega_* \omega_M < 0)$$

($\omega_M \cong CT/eBR$, $\omega_* \cong CT/eBr$.)

STABILITY FOR +VE FEEDBACK

PHASE 180° GAIN: $\epsilon^{1/4} (|\omega_* \omega_M|)^{1/2}$

4

$$n_T = \frac{1}{2\sqrt{\pi}} \left(\frac{1}{T}\right)^{3/2} n(r) \int_T \frac{B d\mu d\mathcal{E}}{|\sqrt{\mathcal{E} - \mu B - q\Phi}|} e^{-\mathcal{E}/T}$$

$$= \frac{n(r)}{T\sqrt{\pi}} \int_{\mu_m}^{\infty} B d\mu \, e^{-(\mu B + q\Phi)/T} \left\{ x_{max} e^{-x^2_{max}} - x_{min} e^{-x^2_{min}} \right\}$$

$$x^2_{\substack{max \\ min}} = \epsilon\lambda \left[ \frac{\mu}{\mu_m} ( \cos\theta - \cos\theta_{\substack{min \\ max}} ) + \frac{q}{|q|} ( \theta - \theta_{\substack{min \\ max}} ) \right]$$

$$\lambda \equiv \mu_m B_o / T$$

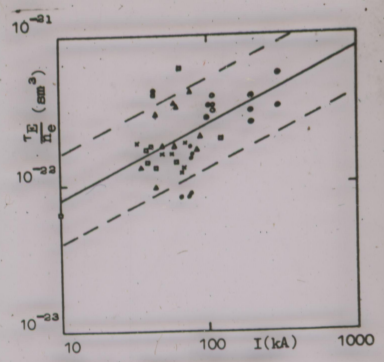


Fig. 3. Type B scaling

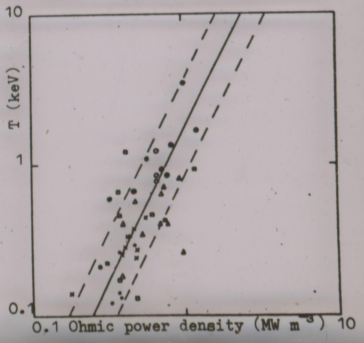


Fig. 4. Type C scaling

2

## ENERGY OF TRAPPED PARTICLES

$$\mathcal{E} = \frac{1}{2} m V_{\parallel}^2 + \mu B + q\Phi$$

PARTICLE TRAPPED IF

$$\mathcal{E} < (\mu B + q\Phi)_{max} \longrightarrow \left[\begin{array}{l}\text{lower maximum} \\ \text{of potentiel}\end{array}\right]$$

MAXIMUM AND MINIMUM OF $(\mu B + q\Phi)$ FOR A GIVEN $\mu$ OCCUR AT

$$\theta_{min} = \mathrm{Sin}^{-1}\left(q E_o R_o / \mu B_\theta\right)$$

$$\theta_{max} = \pi - \theta_{min}$$

SOURCE TERM

$S_F = -i\omega_f \tilde{n}_t$ (FLUID THEORY)

$S_K = -i\omega_f \tilde{n}_t \, \delta(v_{\parallel}) \, \delta(v_{\perp} - v_b) \, \delta(\psi)/2\pi v_{\perp}$

(KINETIC THEORY)

GAIN: AMP($\omega_f$) PHASE: ARG($\omega_f$)

$\omega_f > 0$ −VE FB & VICE VERSA

3

FOR $= \mu = \mu_{min} = qR_0E_0 / B_\theta$,

$\theta_{min} = \theta_{max} = \pi/2$

NO TRAPPING FOR $\mu < \mu_{min}$

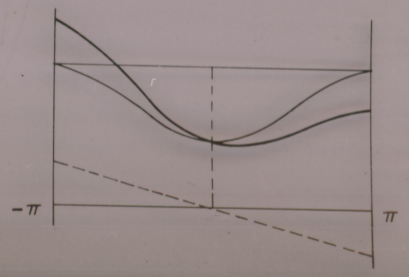

# TRAPPED ELECTRON REGIME

$$\omega_{*e} < \nu_e/\epsilon \quad , \quad (\epsilon T_i/m_i)^{\frac{1}{2}} < \omega/k_{\parallel} < (\epsilon T_e/m_e)^{\frac{1}{2}}$$

$$\omega_R \simeq \omega_{*e} \quad , \gamma \simeq \frac{\epsilon}{\nu_e}^{3/2} \left\{ \omega_{*e} (\omega_f^R + \omega_{*e}) / (1 - \frac{\epsilon}{\nu_e} \omega_f^I) \right\}$$

STABILITY

| | +VE FB | −VE FB |
|---|---|---|
| PHASE | $90^\circ$ | $0^\circ$ |
| GAIN | $\sim \omega_{*e}$ | $\sim \nu_e/\epsilon$ |

7

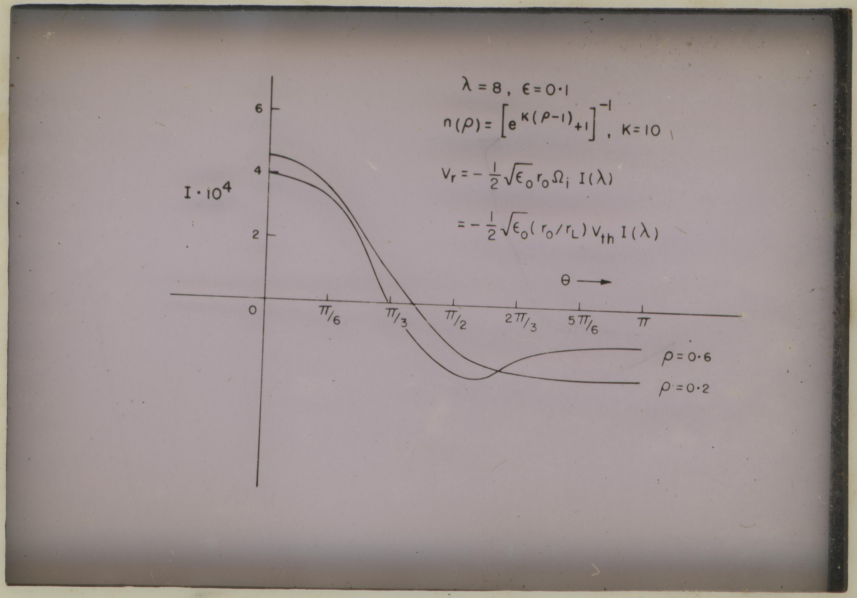
λ = 8, ε = 0·1
n(ρ) = [e^{K(ρ-1)} + 1]^{-1}, K = 10
V_r = -½√ε₀ r₀ Ω_i I(λ)
= -½√ε₀ (r₀/r_L) V_th I(λ)
I · 10^4
6
4
2
0
θ
π/6
π/3
π/2
2π/3
5π/6
π
ρ = 0·6
ρ = 0·2

TABLE I

| Experiment | Main parameters R(m) | a(m) | I(kA) | $n_e(10^{19}m^{-3})$ | Symbol on Graphs | References |
|---|---|---|---|---|---|---|
| T3 and T3a | 1.0 | 0.1-0.17 | 36-90 | 0.9-2.7 | Δ | 1,2 |
| T4 | 1.0 | 0.17 | 110-180 | 1.0-3.0 | o | 3,4 |
| ST | 1.09 | 0.06-0.14 | 10-100 | 0.8-3.3 | □ | 5,6,7,8,9 |
| ATC (uncomp$^d$) | 0.88 | 0.17 | 60-80 | 0.6-2.1 | • | 10,11 |
| ORMAK | 0.8 | 0.23 | 95-160 | 1.2-2.0 | * | 12,13 |
| CLEO-Tokamak | 0.9 | 0.12-0.18 | 34-72 | 1.0-2.4 | x | 14 |
| TFR | 0.98 | 0.17-0.2 | 103-300 | 1.6-3.5 | ⊕ | 15,16 |
| PULSATOR | 0.7 | 0.12 | 44 | 1.1 | ◉ | 17 |
| ALCATOR | 0.54 | 0.10 | 190 | 1.5 | ▽ | 18 |

$$= 8\pi q r_0^2 \int_0^1 \rho' d\rho' \int_{-\pi}^{\pi} d\theta' \left(1+\epsilon_0 \rho \cos\theta\right)^{-1/2} \left(1+\epsilon_0 \rho' \cos\theta'\right)^{-1/2}$$

$$Q_{-1/2}\left[\xi(r, r' \theta, \theta')\right]\left[n^+(r', \theta') - n^-(r', \theta')\right]$$

where $\xi = 1 + \frac{1}{2}\epsilon_0^2 \frac{\rho^2 + \rho'^2 - 2\rho\rho' \cos(\theta - \theta')}{(1+\epsilon_0 \rho \cos\theta)(1+\epsilon \rho' \cos\theta')}$

$\epsilon_0 = \frac{r_0}{R_0}$ , $\rho = \frac{r}{r_0}$ , $\rho' = \frac{r'}{r_0}$

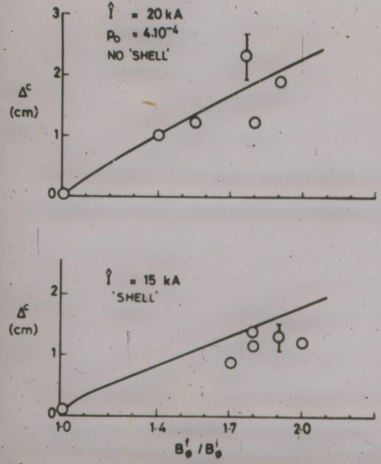


Fig.4 Experimental and theoretical displacements as a result of compression: upper with applied $B_V$; lower with simulated shell

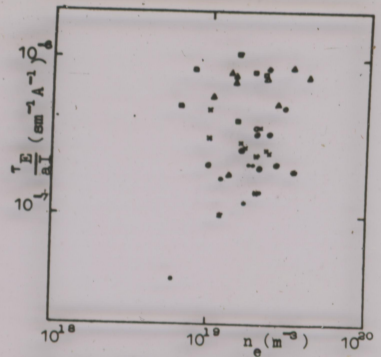


Fig. 2. Type A scaling.

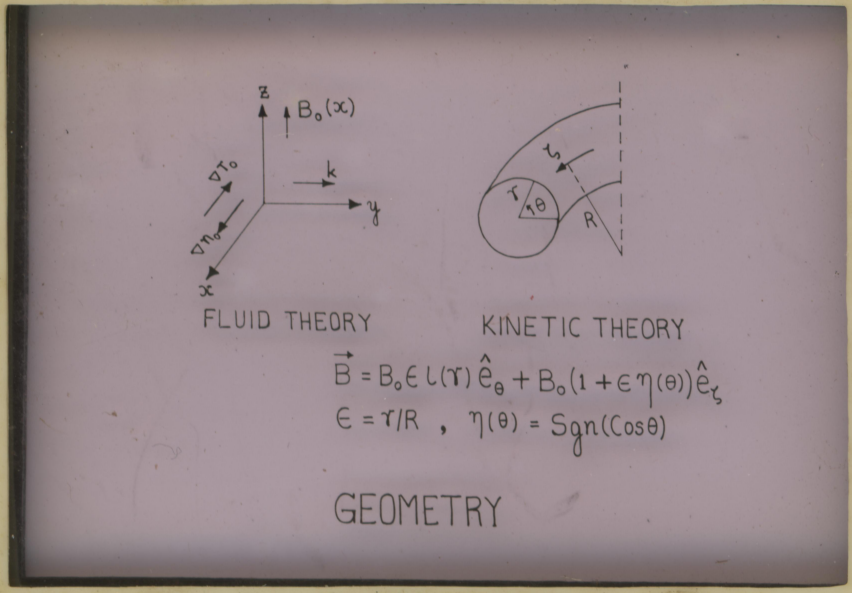
z
$B_0(x)$
k
y
x
$\nabla T_0$
$\nabla n_0$
$r_s$
$r_\theta$
R
FLUID THEORY
KINETIC THEORY
$\vec{B} = B_0 \epsilon \ell(r) \hat{e}_\theta + B_0(1 + \epsilon \eta(\theta)) \hat{e}_\zeta$
$\epsilon = r/R$ , $\eta(\theta) = Sgn(Cos\theta)$
GEOMETRY

## POLARIZATION OF TRAPPED PARTICLES IN A TOKAMAK

$V_r = \frac{cE_\theta B_\phi}{B^2}$ IS RADIALLY INWARDS

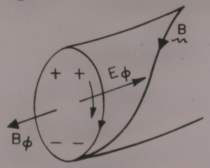


$$\Phi = -\int dl\, E_{\parallel} = -\frac{rB_0E_0}{B_\theta}\ (\theta + 2\epsilon \sin\theta)$$

$$B_\phi = B_0(1+\epsilon\cos\theta)^{-1} \qquad \epsilon = r/R_0$$

## BASIC EQUATIONS

$$\frac{\partial n}{\partial t} + \nabla \cdot (n\vec{v}) = S$$

$$\frac{\partial \vec{v}}{\partial t} + (\vec{v}\cdot\nabla)\vec{v} = \frac{e}{m}\left(-\nabla\varphi + \frac{\vec{v}\times\vec{B}_0}{c}\right) - \frac{1}{mn}\nabla(nT)$$

$$(\tilde{n}_t + \tilde{n}_U)_e = (\tilde{n}_t + \tilde{n}_U)_i$$

FOR UNTRAPPED PARTICLES

$$\tilde{n}_U = n_0(1 - \sqrt{\epsilon})\, e\varphi/T$$

119

(b)

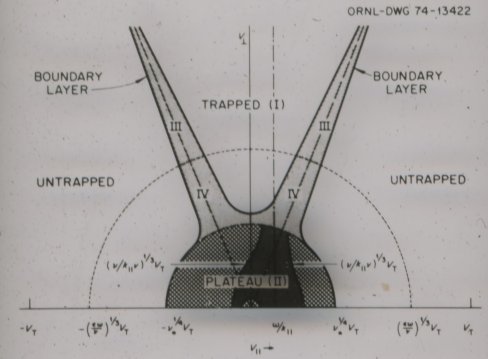


Figure 1 Regimes of collisionality in velocity space as seen on the outside of the torus.

TABLE III

| | | | | |
|---|---|---|---|---|
| I (kA) | 96 | 145 | 200 | 303 |
| V (volts) | 1.85 | 1.85 | 1.75 | 1.88 |
| q (a) | 10 | 7 | 4.8 | 3.3 |
| $N_e l$ ($10^{15} cm^{-2}$) | 1.07 | 1.25 | 1.88 | 2.51 |
| $W_e$ (J/cm) | 2.7 | 5.4 | 8.1 | 13 |
| $W_i$ (J/cm) | 1.6 | 3.1 | 4.5 | 8 |
| $\beta$ | 0.62 | 0.54 | 0.42 | 0.3 |
| $Z_{eff}$ | 3.6 | 4.2 | 2.7 | 3.55 |
| $\tau_E$ (ms) | 15 | 19.5 | 22 | 22.7 |

from Tables I + II

7

## KINETIC EFFECTS

INCLUSION OF MOMENTUM SOURCE &

FLR CORRECTIONS - ALL DISSIPATIVE

INSTABILITIES SIMULTANEOUSLY

SUPPRESSED WITH -VE FB

PHASE $-90^{\circ}$ GAIN $\sim 2\nu_e^2 / 3\epsilon^2 \eta_e \omega_{*e}$

$$= - h^{\xi} \frac{dp}{d\psi} - \frac{f(\psi)}{h^{\xi}} \frac{df}{d\psi} \quad , \qquad (5)$$

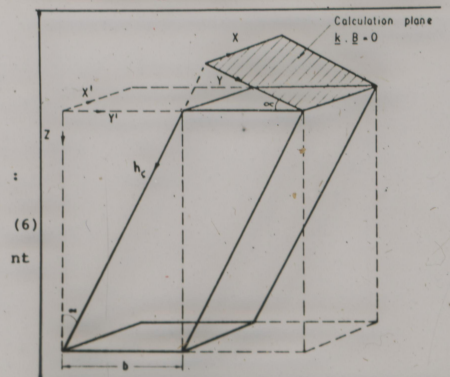


:

(6)

nt

ly,

**Fig.1** Slab model with periodic 'toroidal' (z) and 'poloidal' (y') directions. With a rational surface, the field vanishes in one of the planes containing a wave-number.

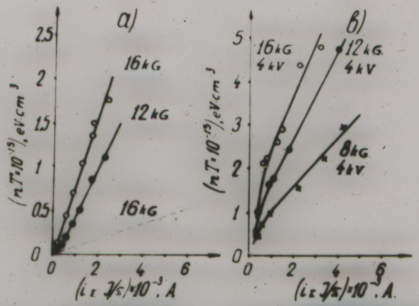


Fig.1. $nT(\int E\,dt)$, dotted line corresponds to Artsimovich's formula with $C^2 = 5$.

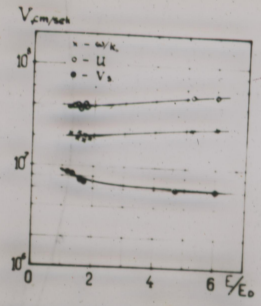


Fig.2. $n = 3 \div 5 \cdot 10^{13}$
$B$ =16 KG

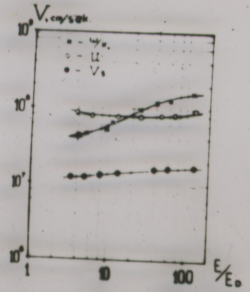


Fig.3. $n = 4 \cdot 10^{12} cm^{-3} - 2 \cdot 10^{13}$
$B$ =16 KG

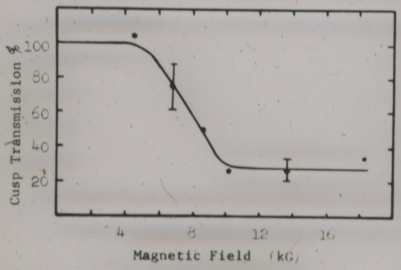


Fig.1. Cusp Transmission

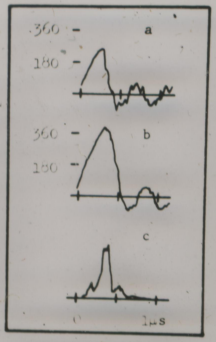


Fig.2. Diode voltage in kV, (a) without and (b) with iron collar; (c)

| Machine | 100 kV Marx | 500 kV, 7 Ω Blumlein | 150 kV Blumlein | 5 MV CREB |
|---|---|---|---|---|
| Ion Energy | ~ 100 keV | 300 keV | 130 keV | 2 MeV |
| Ion Current | 2 x 250 A | 2 x 2,050 A | 2 x 3,300 A | ~ 5,000 A |
| Pulse Width | ~ 50 nsec | ~ 50 nsec | ~ 50 nsec | ≤ 50 nsec |
| Current Density | ~ 10 A/cm$^2$ | 8.3 A/cm$^2$ | ~ 20 A/cm$^2$ | ~ 30 A/cm$^2$ |
| Efficiency $\eta$ | | 9% | 42% | |
| Type of Ions | proton | proton | proton | proton & $Al^{++}$ |

TABLE I - $\eta$ = Proton Energy/Total Energy Input $\int VIdt$

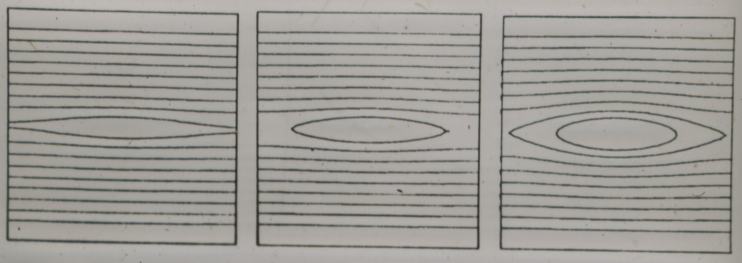

Fig.2. The non-linear evolution of an island state (left to right) for a symmetric Gaussian distribution. The final equilibrium state ($\delta E=0$) is illustrated on the right.

C. Example or Solutions. The non-linear development of the instability, with the final island state ($\delta E = 0$) is illustrated in Fig. 2.

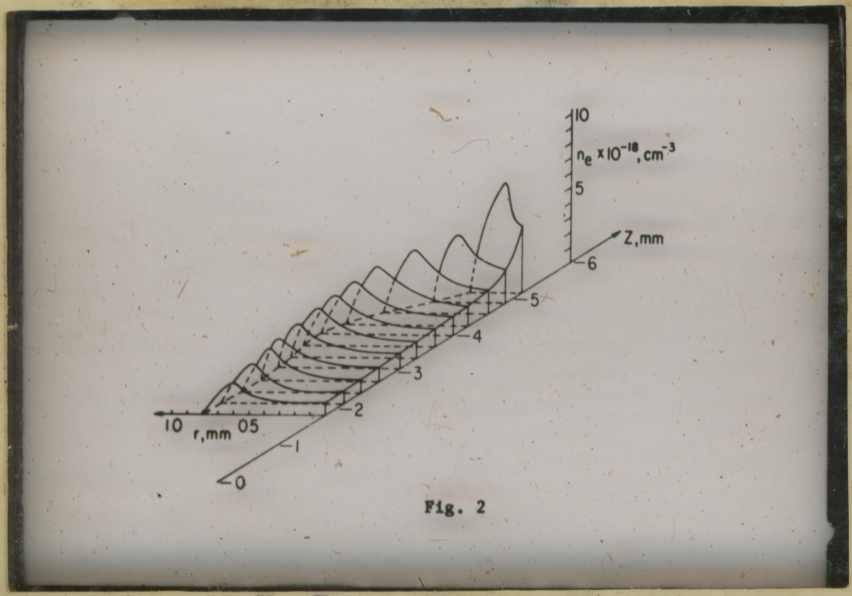


Fig. 2

plasma in a field of 19.4 kG. The ~30% axial density minimum is much more than

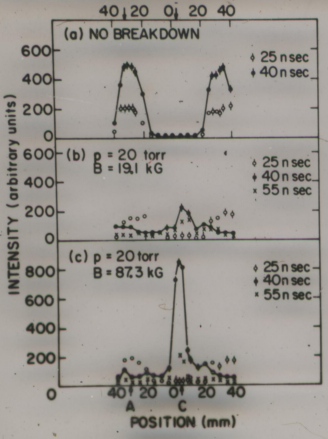


Figure 1

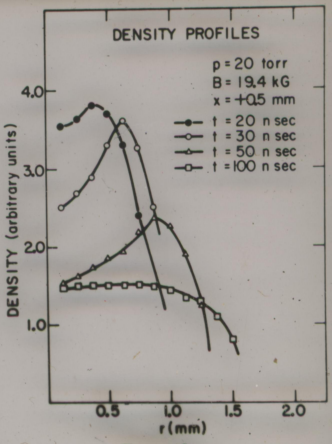


Figure 2

(1)

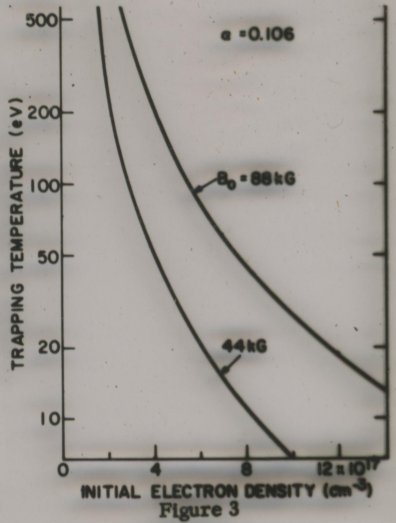
a = 0.106
$B_0$ = 88 kG
44 kG
TRAPPING TEMPERATURE (eV)
500
200
100
50
20
10
0
4
8
12 x $10^{17}$
INITIAL ELECTRON DENSITY ($cm^{-3}$)

Figure 3

12

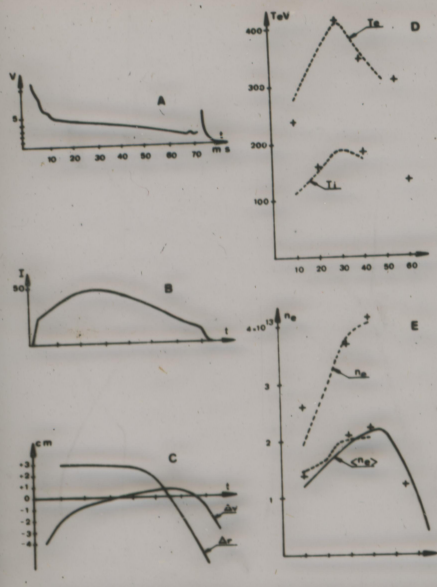


Fig. 1 - A typical 50 kA discharge ; A) loop voltage, B) plasma current, C) radial and vertical displacement, D) electron and ion temperature : + experimental results (Thomson scattering and Doppler broadening of $O_{VII}$ line), E) peak and average electron densities + Thomson scattering results ; solid line : 2 mm interferometry.
On d and e, dashed line are discharge simulation results.

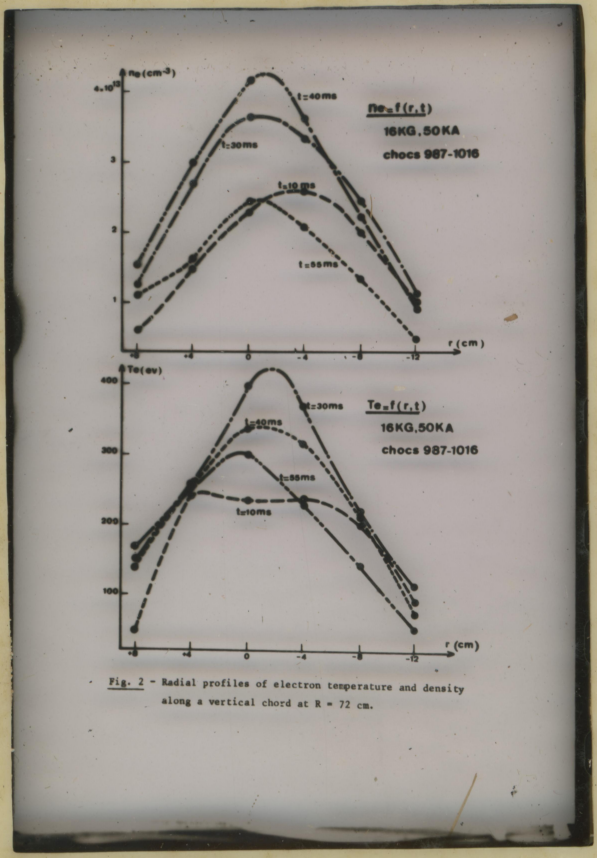


Fig. 2 - Radial profiles of electron temperature and density along a vertical chord at R = 72 cm.

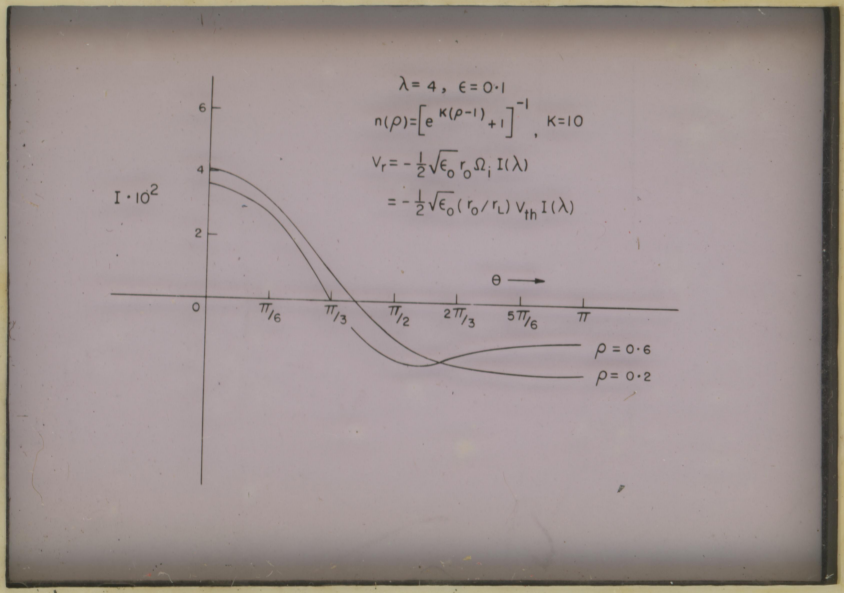
λ = 4 , ε = 0·1
n(ρ) = [e^{K(ρ-1)} + 1]^{-1} , K = 10
V_r = -½√ε_0 r_0 Ω_i I(λ)
= -½√ε_0 (r_0 / r_L) V_th I(λ)
I · 10^2
6
4
2
0
θ
π/6
π/3
π/2
2π/3
5π/6
π
ρ = 0·6
ρ = 0·2

71

DIAGRAM 1

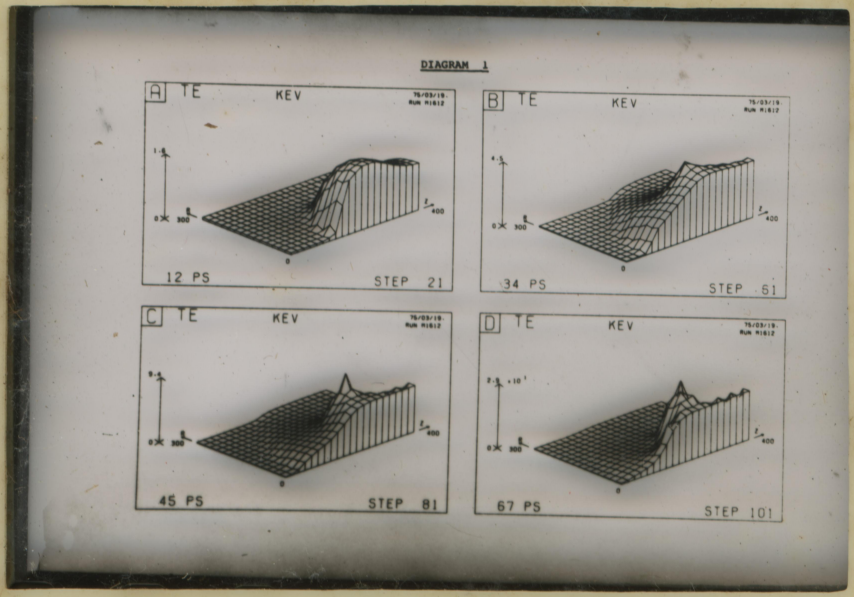
A TE KEV
12 PS
STEP 21
B TE KEV
34 PS
STEP 61
C TE KEV
45 PS
STEP 81
D TE KEV
67 PS
STEP 101

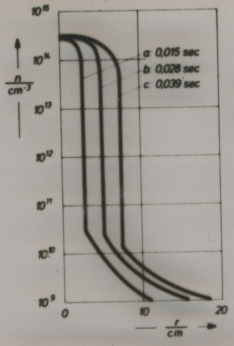


Fig.4: Development of plasma density in time. Beam like in Fig.3b.

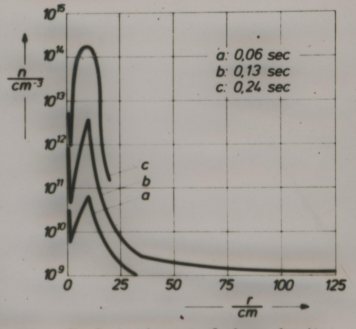


Fig.5: Development of plasma density in time. Beam like in Fig.3c.

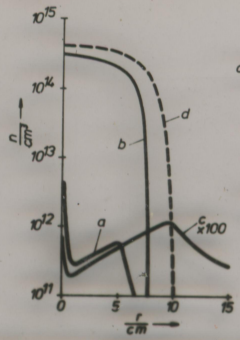


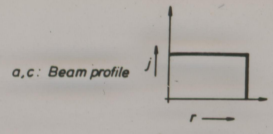


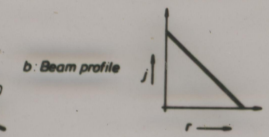


Fig.3: Plasma density distribution after 0.04 sec of injection.

a. Beam with 5 cm radius, constant current density j.

b. Beam with 5 cm radius, current density j peaked on the axis.

c. Beam with 10 cm radius, constant current density j.

d. Pencil beam (case 7 of (1)).

netic field on both particles and (particle) energy.

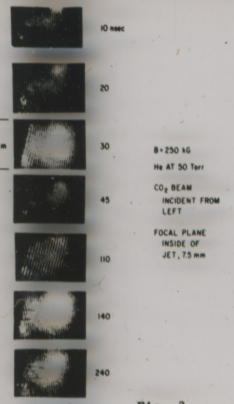


Fig. 3

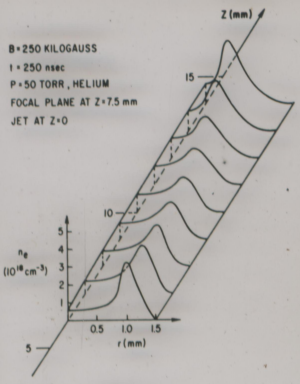


Fig. 4

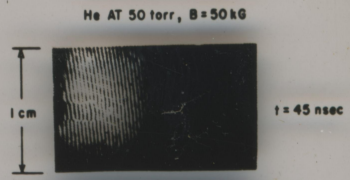


Fig. 1

DIAGRAM 2

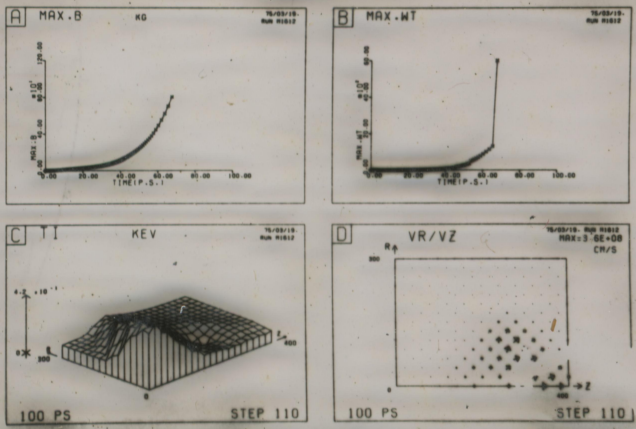
A
MAX.B
KG
TIME(P.S.)
B
MAX.WT
TIME(P.S.)
C
TI
KEV
100 PS
STEP 110
D
VR/VZ
MAX=3.6E+08
CM/S
R
Z
100 PS
STEP 110

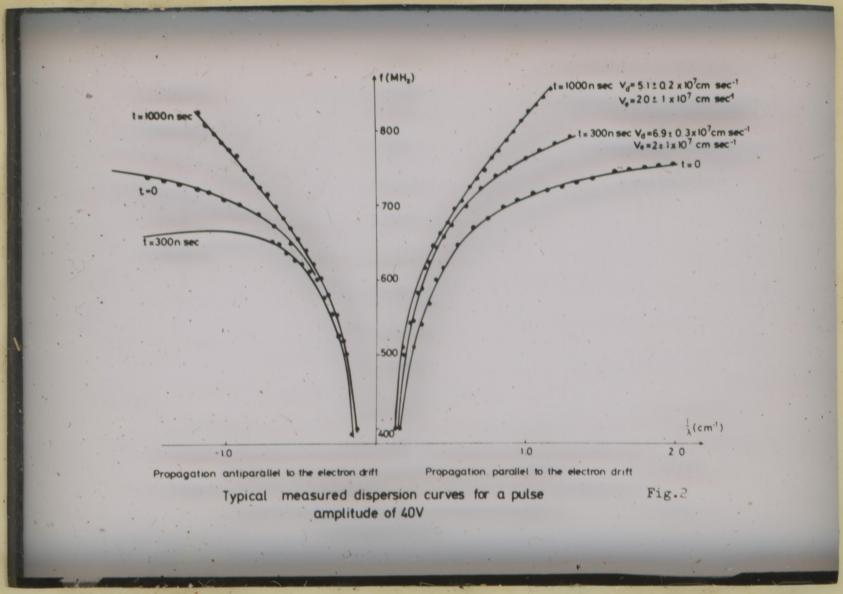


Typical measured dispersion curves for a pulse amplitude of 40V

Fig.2

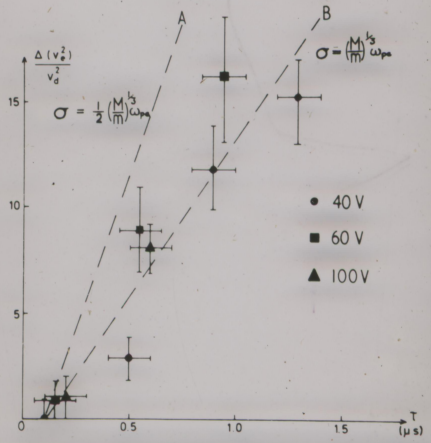


Estimation of the electrical conductivity, $\sigma$, from the electron heating rate

Fig.5

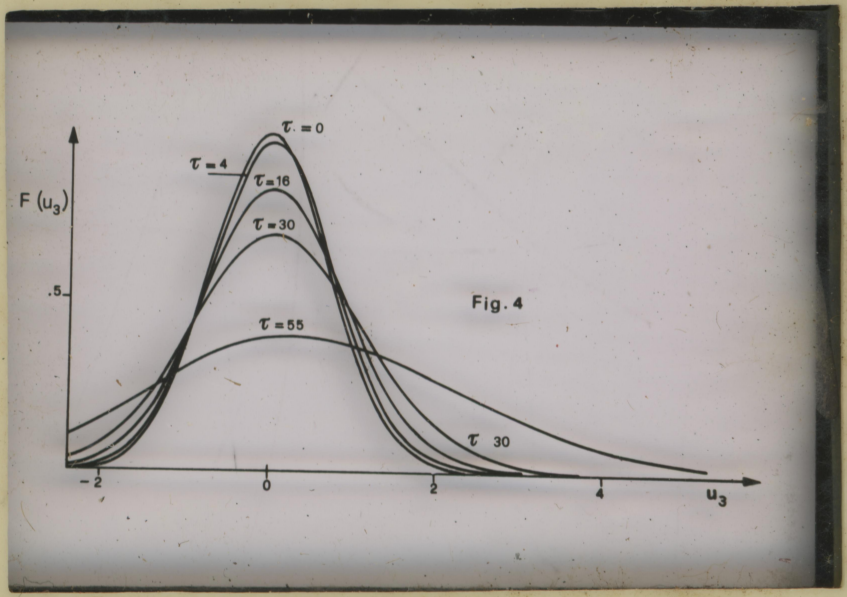


Fig. 4

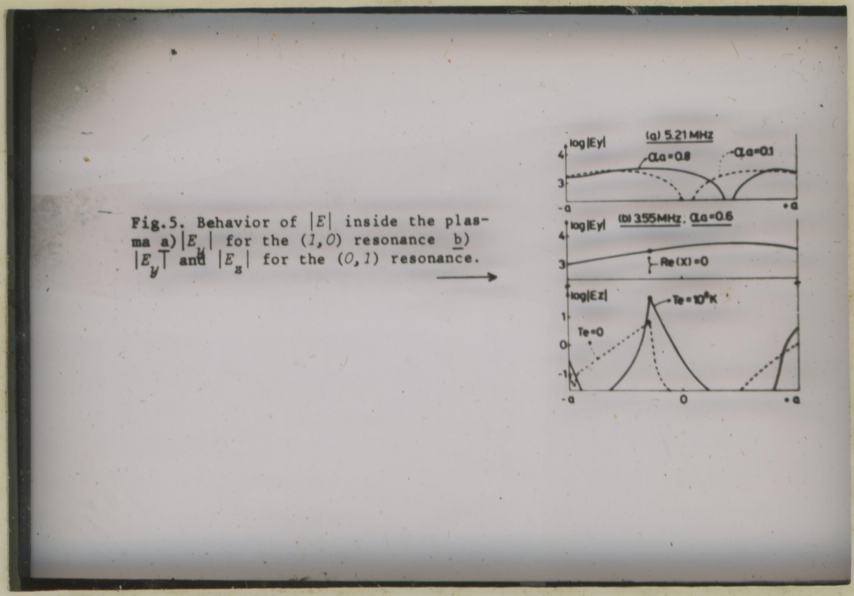


Fig.5. Behavior of $|E|$ inside the plasma a) $|E_y|$ for the $(1,0)$ resonance b) $|E_y|$ and $|E_z|$ for the $(0,1)$ resonance.

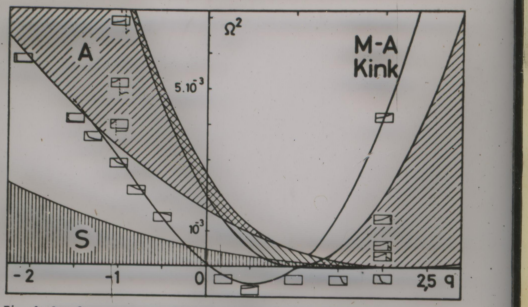


Fig. 1: Low-frequency part of the m=1 spectrum of a screw-pinch. S = slow-wave continuum, A = Alfvèn continuum. Singly hatched region = one singularity, doubly hatched region = two singularities. M.A. = magne-to-acoustic.The internal kink is barely visible between q=1 and q=2.3. The radial component of the eigenvector is shown in the rectangles, the center being on the left.

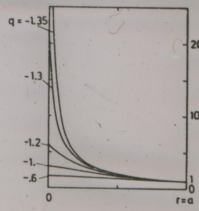


Fig. 2: Radial component of the eigenvector normalized to its boundary-value, for values of q on both sides of the merging point. At q=-1.35 the kink has already reached the continuum.

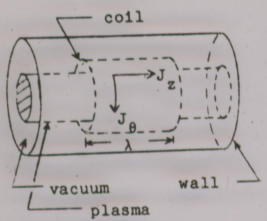
coil
$J_z$
$J_\theta$
λ
vacuum
plasma
wall

Fig. 1

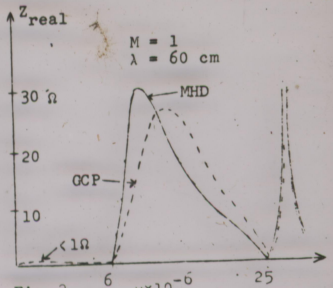
$Z_{real}$
M = 1
λ = 60 cm
30 Ω
20
10
MHD
GCP
<1Ω
6
25
ω×10⁻⁶

Fig. 2

Main results of our experiments are given in figures.

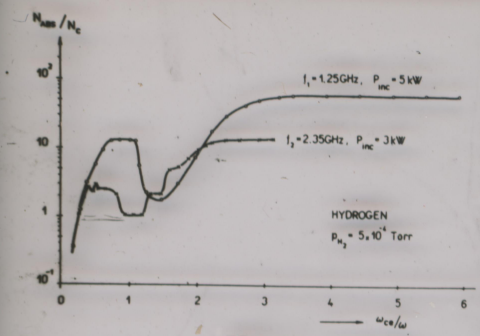


FIG. 1

Fig. 1 shows the dependence of a mean electron density $N_{abs}$ of the hydrogen plasma created after absorption of the microwave power with frequency $f_1$ = 1.25GHz and $f_2$ = = 2.35GHz in the initial plasma on the magnetic field $\omega_{ce}/\omega$. Since the degree of ionization of our initial plasma was very small ($\lesssim 1\%$) and practically all the absorbed energy went into neutral gas ionization,

by nonlinear wave-wave interaction

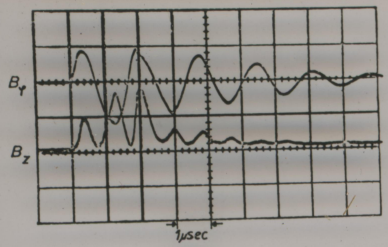


Fig. 1 : $B_\varphi$ and $B_z$ at r = 8 mm

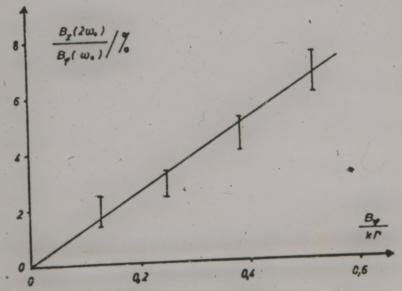


Fig. 2: Amplitude of double frequency $B_z$ as a function of $B_\varphi$

In the low amplitude case, the Alfvé

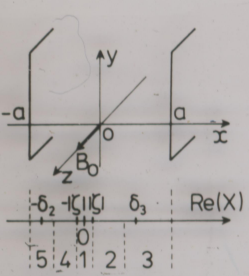


Fig.3. Slab with coordinate systems ($-\delta_2$ and $\delta_3$ correspond to $\omega_{S2}=\omega$ and $\omega_{S3}=\omega$).

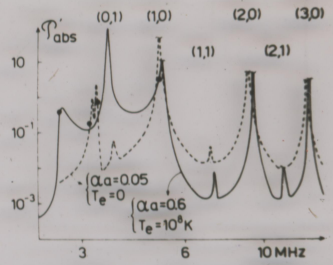


Fig.4. $\mathcal{P}'_{abs}$ for an inhomogeneous slab with $\alpha a=0.05$ and $\alpha a=0.6$. The dots indicate where $Re(X)=0$ coincides with $x=\pm a$.

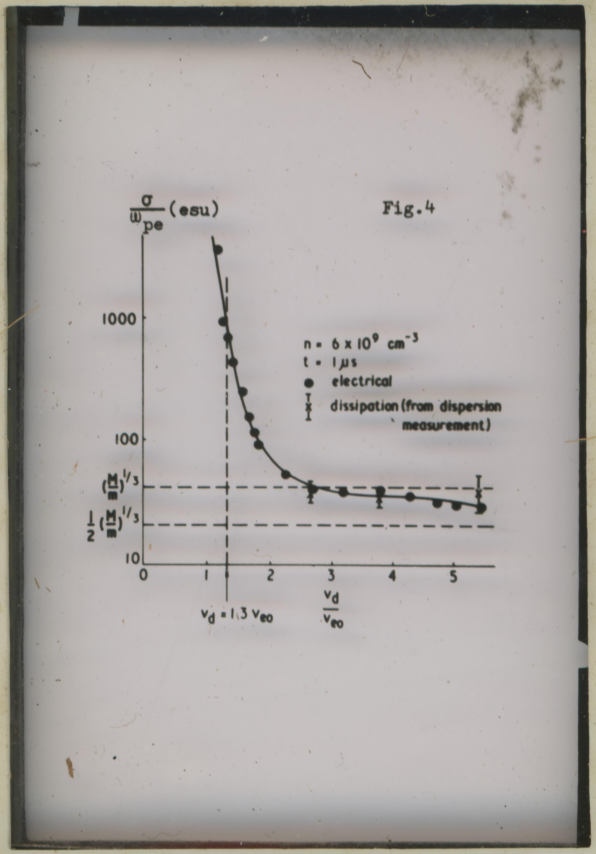
$\frac{\sigma}{\omega_{pe}}$ (esu)
1000
100
$(\frac{m}{8\pi M})^{1/3}$
$\frac{1}{2}(\frac{m}{8\pi M})^{1/3}$
10
0
1
2
3
4
5
$\frac{v_d}{v_{eo}}$
$v_d = 1.3\, v_{eo}$
n = 6 x 10⁹ cm⁻³
t = 1 μs
electrical
dissipation (from dispersion measurement)

Fig. 4

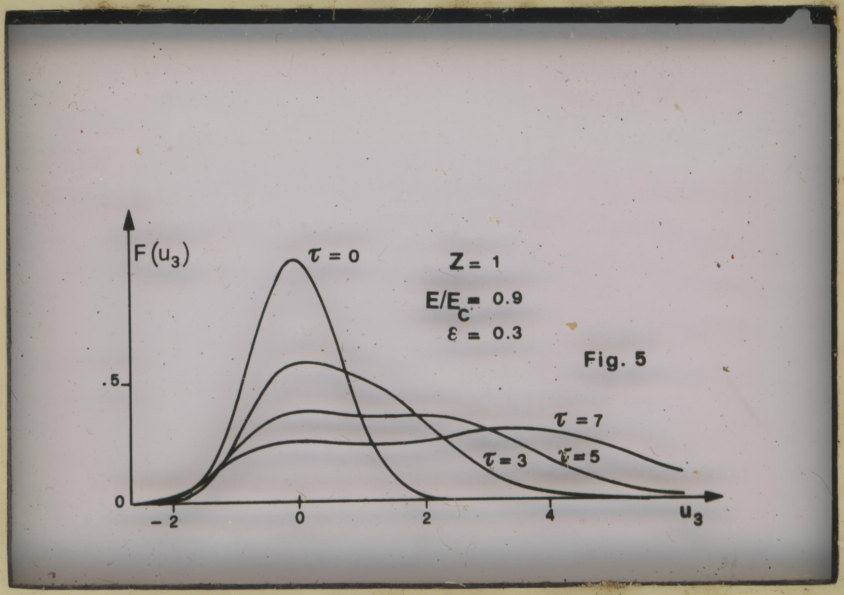


Fig. 5

144

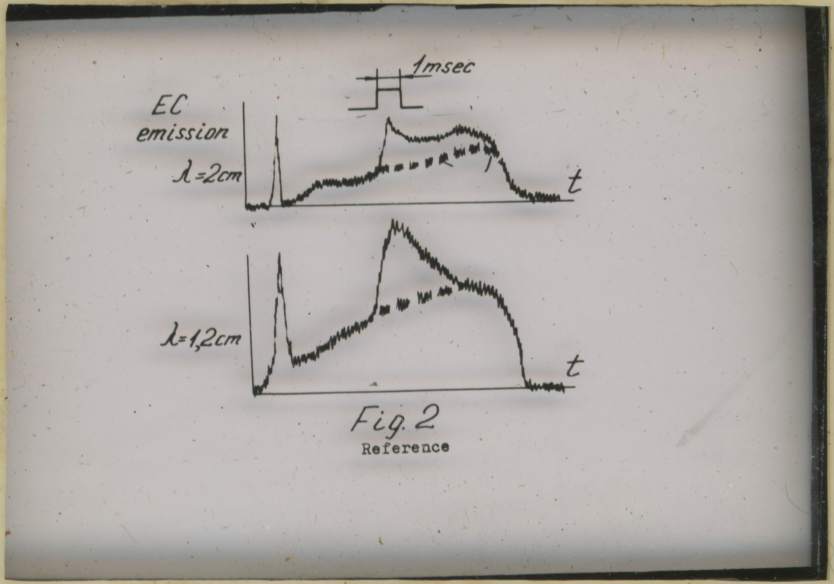


Fig. 2
Reference

Fig. 1

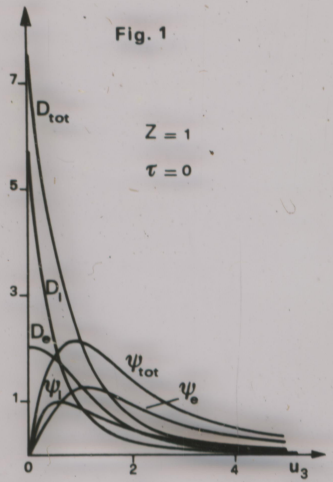

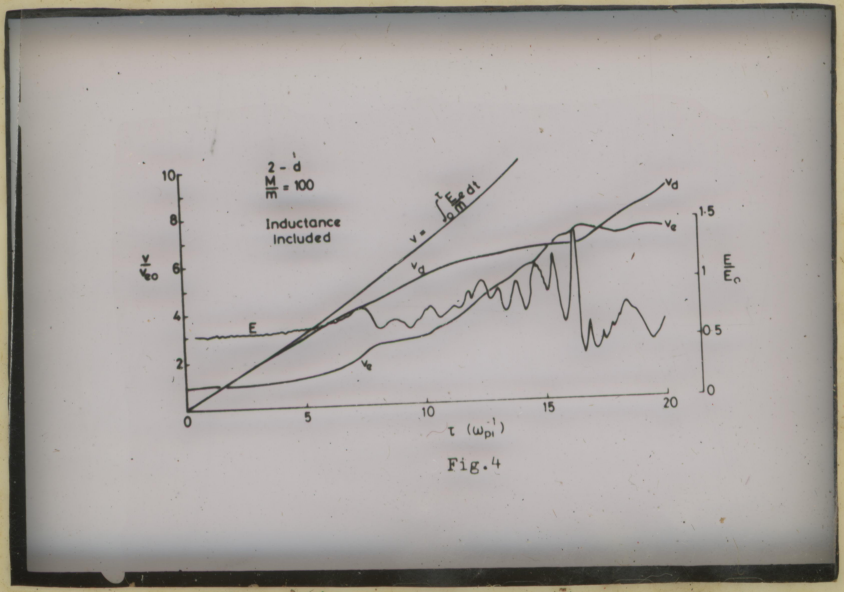
2 - d
M/m = 100
Inductance
Included
v = ∫ E dt
v_d
v_e
E
10
8
6
4
2
0
5
10
15
20
1·5
1
0·5
0
v/v_eo
E/E_c
τ (ω_pi^-1)

Fig.4

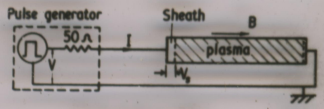


$$V = V_s + R_p I + 50I$$

$$V_s \propto I^{2/3}$$

(a) Schematic arrangement of the experiment

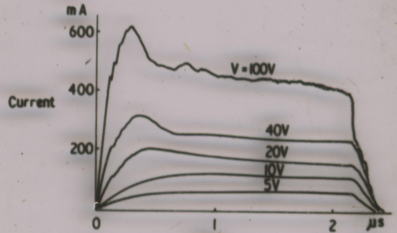


(b) Plasma current Fig.1

153

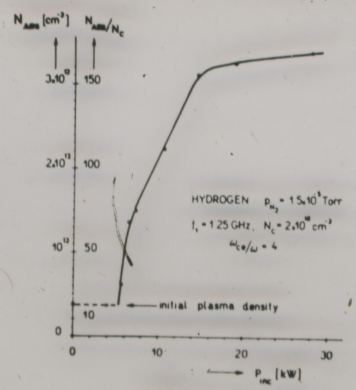
$N_{Abs}$ [cm$^{-3}$]
$N_{Abs}/N_c$
$3\times10^{12}$
150
$2\times10^{12}$
100
$10^{12}$
50
0
10
initial plasma density
0
10
20
30
$P_{inc}$ [kW]
HYDROGEN $p_{H_2} = 1.5\times10^{-1}$ Torr
$f_0 = 1.25$ GHz, $N_c = 2\times10^{11}$ cm$^{-3}$
$\omega_{Ce}/\omega = 4$

FIG. 3

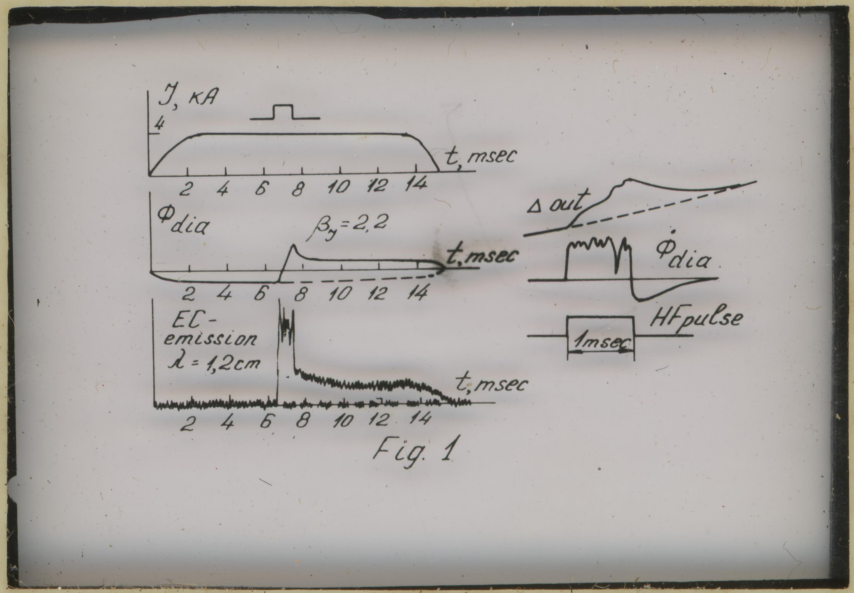
J, kA
4
t, msec
2 4 6 8 10 12 14
Φdia
βy=2,2
t, msec
2 4 6 8 10 12 14
EC-
emission
λ = 1,2cm
t, msec
2 4 6 8 10 12 14
Δ out
Φdia
HF pulse
1msec

Fig. 1

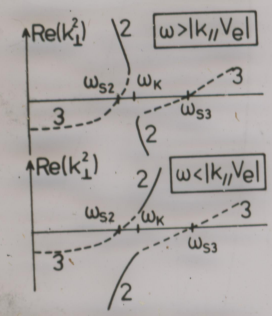


Fig.1. $k_{\perp 2}^2$ and $k_{\perp 3}^2$ versus $\omega$.

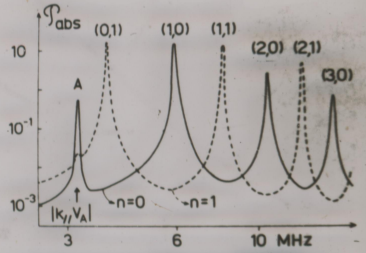


Fig.2. Spectra for $n=o$ and $n=1$ in the homogeneous cylindrical case (radius $=a$ , $T_e = o$).

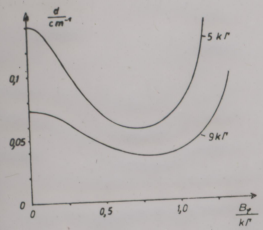


Fig. 3:
Damping constant d ( $B_\varphi \propto e^{-dz}$ ) as a function of the amplitude $B_\varphi$

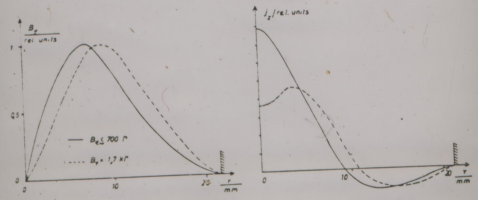


Fig. 4:
Normalized radial amplitude profile $B_\varphi$ and connected current density $j_z$ for two different wave amplitudes.

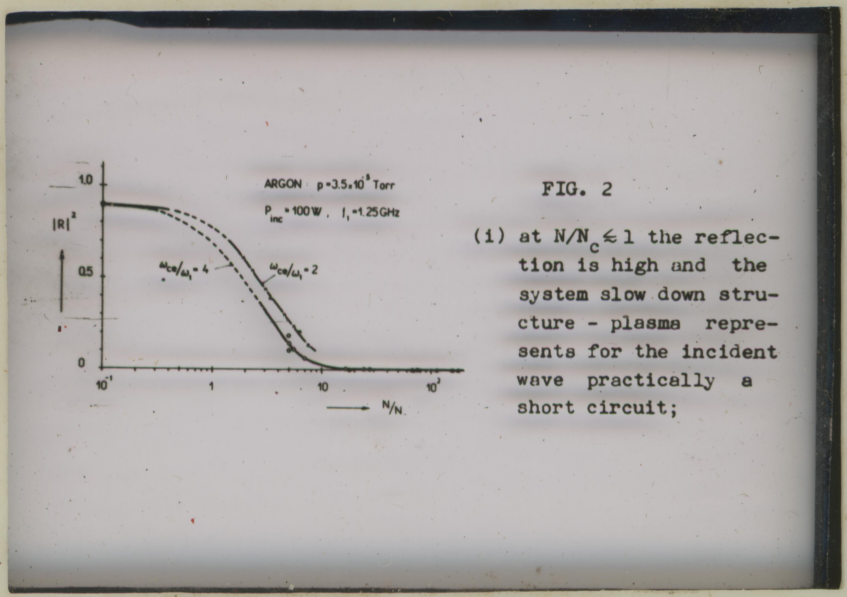


FIG. 2

(i) at $N/N_c \leq 1$ the reflection is high and the system slow down structure - plasma represents for the incident wave practically a short circuit;

radial direction we do not find a clear phaseshift. In azimuthal direction the phaseshift corresponds to a phasevelocity of $8 \times 10^3$ m/s in the ion-gyration direction.

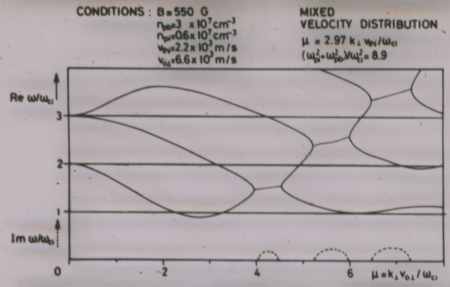


**Fig.3** Dispersion of perpendicular propagating ion cyclotron waves in a plasma with a velocity distribution which consists of a mixture of a Maxwellian and a $\delta$-function. Low B-field case.

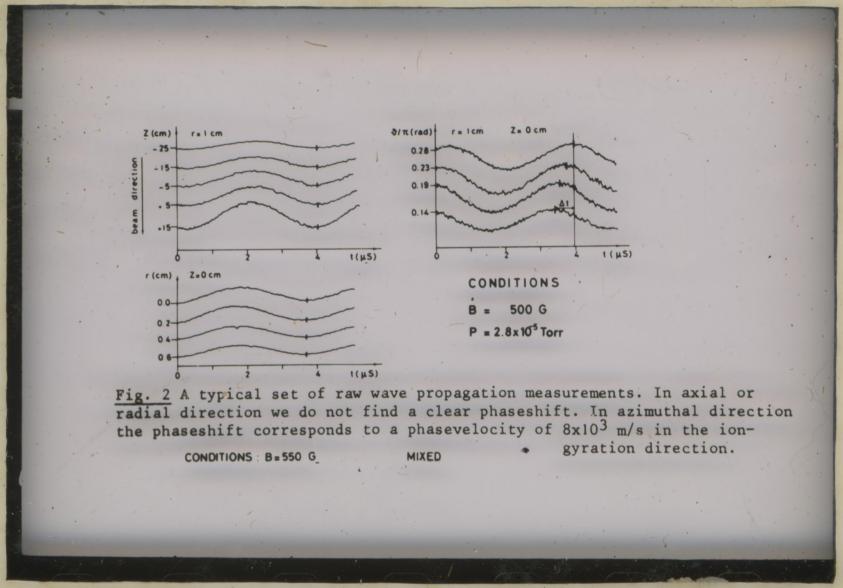


Fig. 2 A typical set of raw wave propagation measurements. In axial or radial direction we do not find a clear phaseshift. In azimuthal direction the phaseshift corresponds to a phasevelocity of $8 \times 10^3$ m/s in the ion-gyration direction.

CONDITIONS : B=550 G MIXED

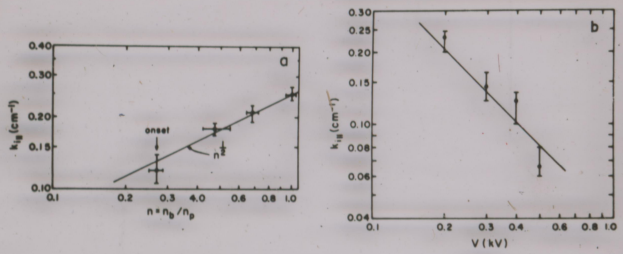


Fig. 3: (a) Beam density dependence ($V_b$ = 200 V), and (b) Beam energy dependence ($n_b \sim 10^8 cm^{-3}$) of the spatial growth rate B = 4 kG, $n_p = 3 \times 10^8 cm^{-3}$.

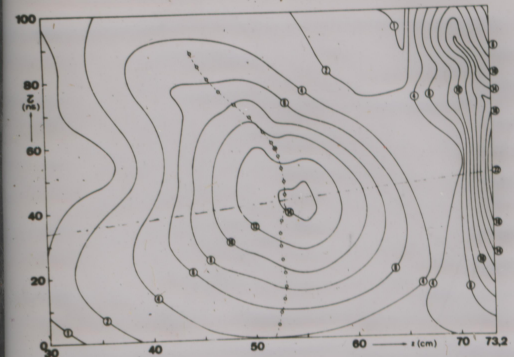


Fig. 2 - Space-time analysis of the instability electric field.

181

(a)

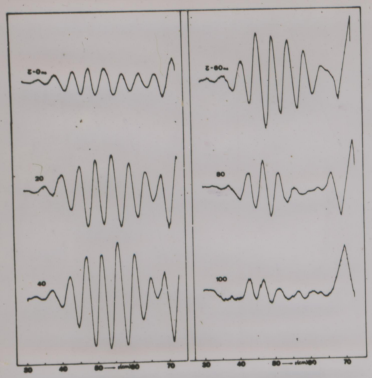

Fig. 1 - "Instantaneous pictures" of the bursts in space.

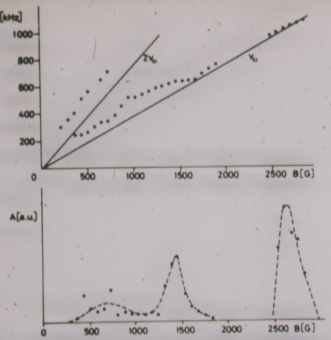


Fig. 1 Dependence of instability frequency and amplitude on the magnetic field.

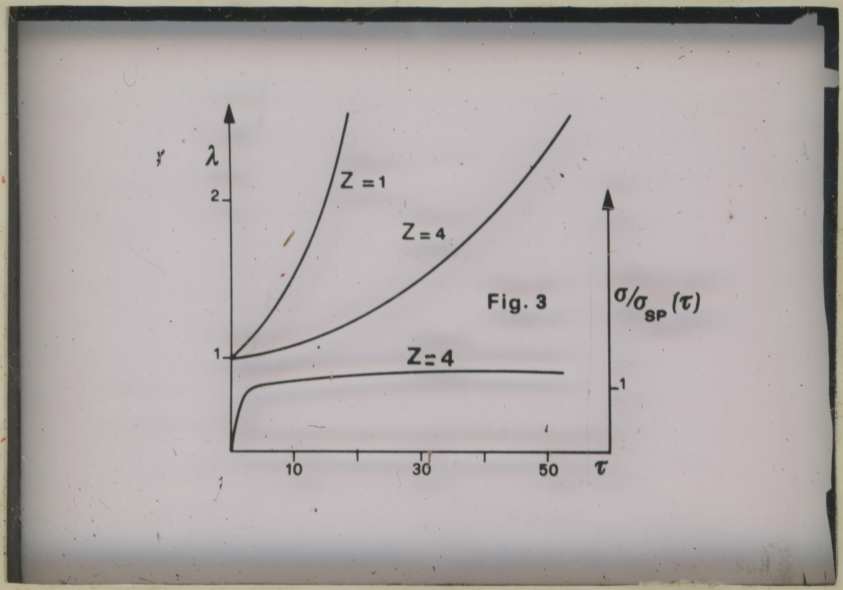


Fig. 3

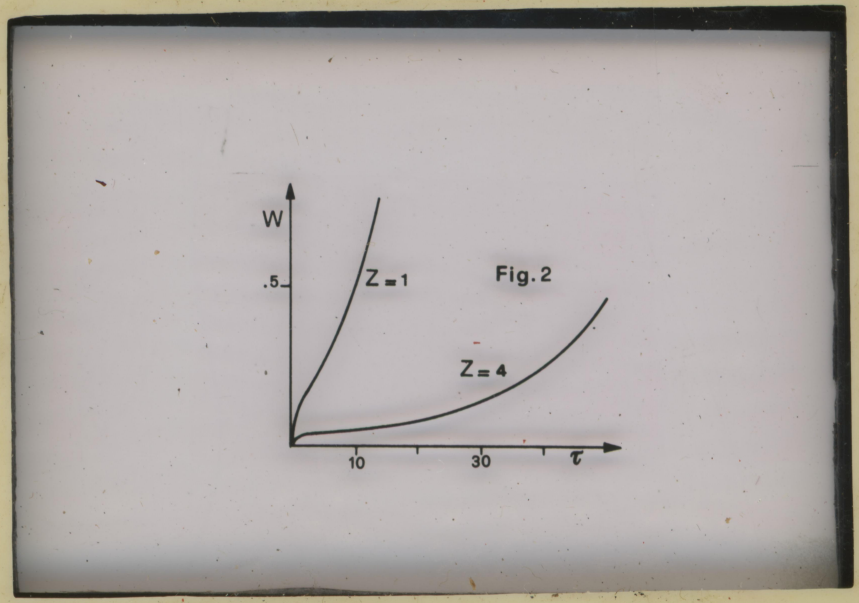


Fig. 2


Fig. 3 - Space-time analysis of the plasma "density". Darker areas represent higher "densities".

(D)

181

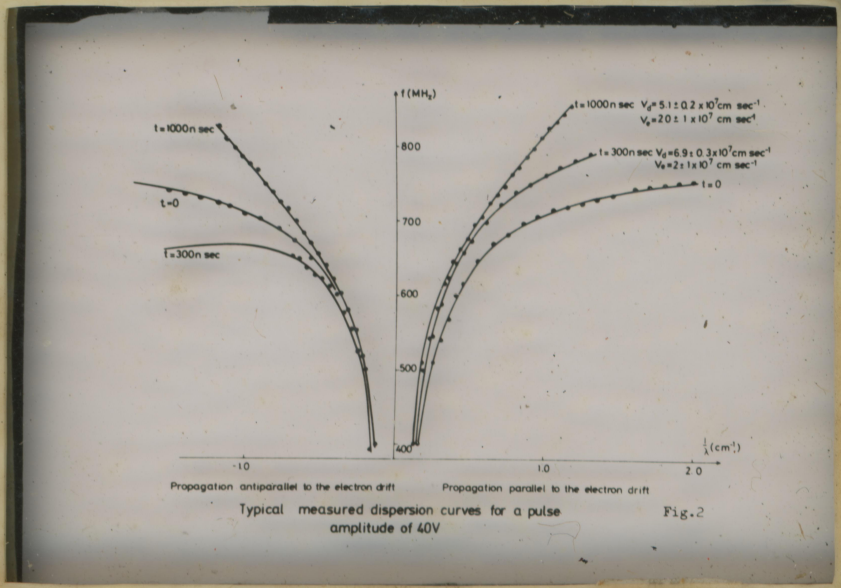


Typical measured dispersion curves for a pulse amplitude of 40V

Fig.2

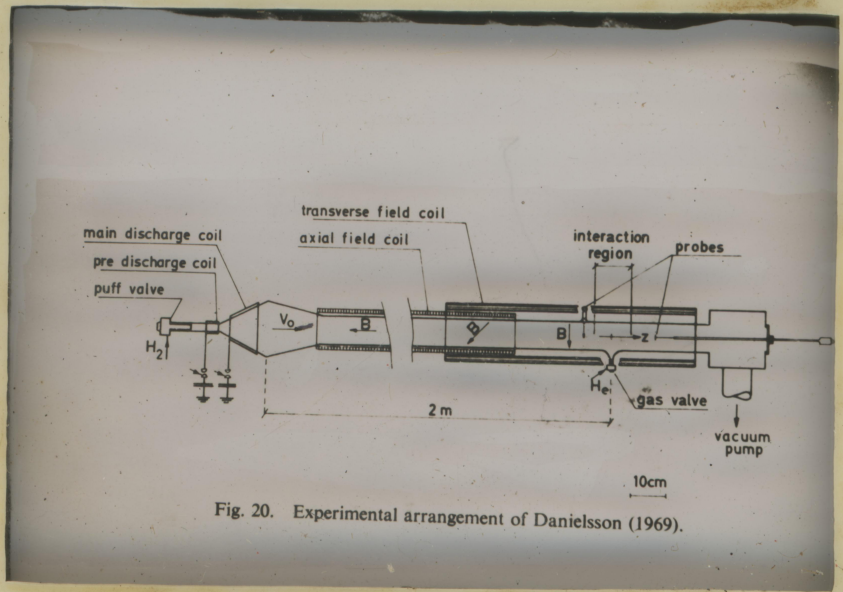


Fig. 20. Experimental arrangement of Danielsson (1969).

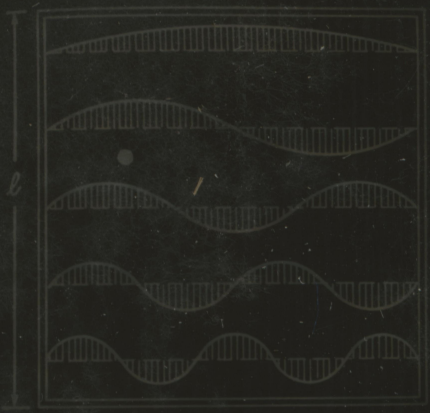


Fig. 23-1. A cross-section of "Jeans's cube," showing the different waves that can exist inside it. Only the waves propagating in a horizontal direction are shown here. The black dot is a tiny coal dust particle.

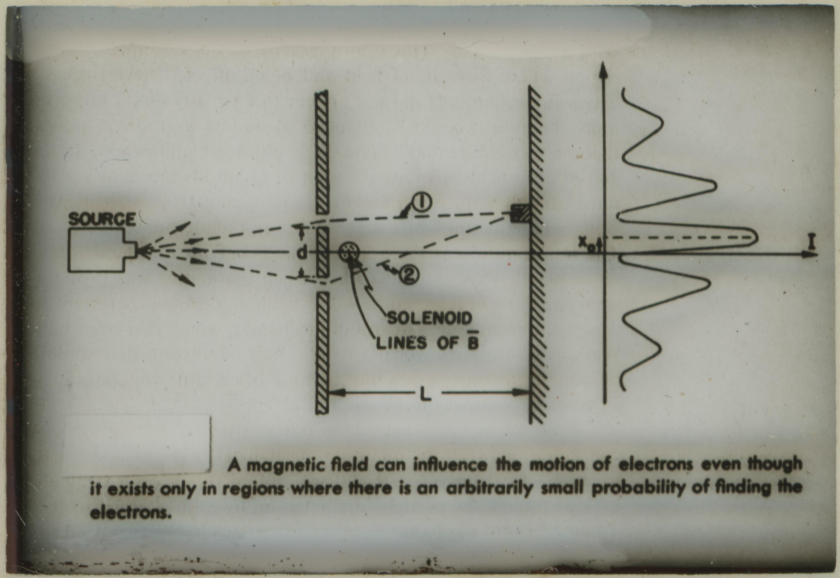


A magnetic field can influence the motion of electrons even though it exists only in regions where there is an arbitrarily small probability of finding the electrons.

If $nA\ell\,\overline{\delta\varepsilon} = dU$ , change in internal energy

$nm\overline{v^2} = p$ , $A\delta\ell = \delta V$

and if

$$\boxed{\delta Q \equiv nV\overline{\delta q}}$$

then

$$dU = \delta Q - p\delta V, \Longrightarrow \text{1st Law}$$

**New Definitions of Heat and Work:**

Work: All that energy added adiabatically

Heat: All that energy added nonadiabatically.

- generalized definitions of heat,

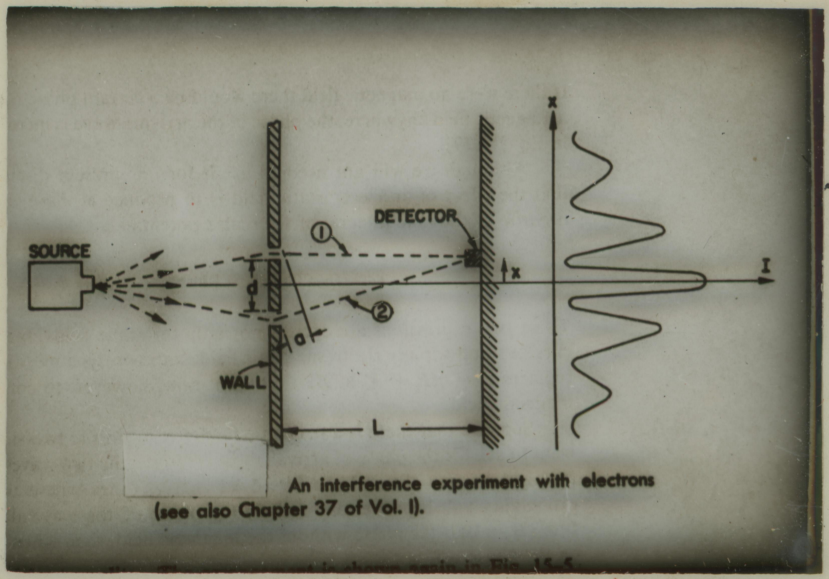


An interference experiment with electrons (see also Chapter 37 of Vol. I).

JET

Experimental Programme:

Phase I :(Starts 1980) 2-3 years

(a) establish a range of operating conditions

(b) perform scaling studies

(c) work upto the maximum of plasma current for the installed power supplies including the use of D-shaped cross-section.

(d) examine additional heating without internal structures.

(e) investigate impurity effects

(f) establish the limits of operation

(g) decide on future power supplies

(h) decide whether diverter is needed

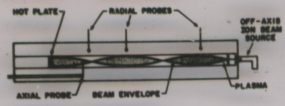


Fig. 1: Schematic of Q-machine and ion beam setup.

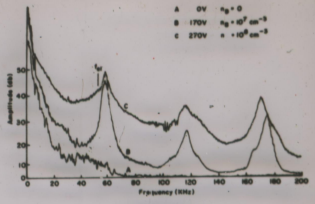


Fig. 2: Frequency spectrum of the mode amplitudes. B = 4.65 kG, $n_p = 3 \times 10^8 cm^{-3}$